

# Variations in surface and electrical properties of polytetrafluoroethylene film after plasma-induced grafting of acrylic acid

Rong Li<sup>1</sup> · Xin-Zhong He<sup>1,2</sup> · Qian-Hong Gao<sup>1,2</sup> · Li-Juan Pang<sup>1,2</sup> · Hong-Long Wang<sup>1,2</sup> · Jiang-Tao Hu<sup>1</sup> · Zhe Xing<sup>1</sup> · Guo-Zhong Wu<sup>1,3</sup>

Received: 17 December 2015 / Revised: 1 March 2016 / Accepted: 2 March 2016 / Published online: 11 May 2016  
© Shanghai Institute of Applied Physics, Chinese Academy of Sciences, Chinese Nuclear Society, Science Press China and Springer Science+Business Media Singapore 2016

**Abstract** Polytetrafluoroethylene (PTFE) film was graft-polymerized with acrylic acid (AAc) via a low-temperature plasma technique. The effect of plasma treatment parameters (radio-frequency power and treatment time) on the spin number of free radicals in PTFE film was examined. Attenuated total reflection Fourier transform infrared (ATR-FTIR) spectroscopy, X-ray photoelectron spectroscopy, scanning electron microscopy, and atomic force microscopy were employed to characterize the chemical structure, surface composition, and microstructure of the original PTFE and PTFE-g-PAAc films, respectively, in order to verify the successful graft polymerization of AAc onto a PTFE film surface. Thermogravimetric analysis illustrated that the thermal stability of bulk PTFE film remains unchanged after graft modification. Water contact angle measurements confirmed that the hydrophilicity of PTFE-g-PAAc film was effectively improved as compared to the original PTFE film. The dielectric constant ( $\epsilon_r$ ) of PTFE-g-PAAc ( $GD = 218 \mu\text{g}/\text{cm}^2$ ) film remained invariable, compared to that of the unmodified PTFE film. Nevertheless, the dielectric loss ( $\tan\delta$ ) of PTFE film increased considerably, from 0.0002 ( $GD = 0 \mu\text{g}/\text{cm}^2$ ) to 0.0073 ( $GD = 218 \mu\text{g}/\text{cm}^2$ ), which

might be due to the increase in surface polarity and moisture resulting from AAc graft modification. In addition, the surface electrical resistance ( $R_s$ ) of PTFE film decreased slightly, from 131.89 ( $GD = 0 \mu\text{g}/\text{cm}^2$ ) to 110.28  $\Omega \text{ cm}^2$  ( $GD = 218 \mu\text{g}/\text{cm}^2$ ) after surface modification, but still retained its inherent high impedance.

**Keywords** Polytetrafluoroethylene film · Low-temperature plasma · Acrylic acid · Hydrophilicity · Electrical properties

## 1 Introduction

Polytetrafluoroethylene (PTFE), as one of the most important polymeric engineering materials, is widely applied in numerous fields due to its low frictional coefficient; outstanding chemical, thermal, mechanical, and corrosion resistances; and high electrical resistance [1]. However, the application of PTFE is seriously limited in some areas due to its hydrophobicity, poor compatibility, and low adhesion to other materials. In view of this, it is important to improve its surface properties for specific applications.

Surface modification by molecular design is one of the most versatile methods to anchor functional groups onto polymers for improvement of wettability, biocompatibility, conductivity, lubricity, and adhesive performance [2–4]. PTFE is an ideal material for microelectronics applications owing to its excellent dielectric properties. Many studies have been carried out via different modification techniques in order to activate a PTFE surface and improve the adhesion between a PTFE surface and diverse metals or epoxy resin. A wet chemical treatment, such as that using sodium naphthalene, not only influences the surface

This work was supported by the National Natural Science Foundation of China (Nos. 11275252 and 11305243).

✉ Guo-Zhong Wu  
wuguozhong@sinap.ac.cn

<sup>1</sup> Shanghai Institute of Applied Physics, Chinese Academy of Sciences, Shanghai 201800, China

<sup>2</sup> University of Chinese Academy of Sciences, Beijing 100049, China

<sup>3</sup> School of Physical Science and Technology, Shanghai Tech University, Shanghai 200031, China

performance of PTFE, but also damages its bulk properties. Gamma-ray and electron beam irradiation will induce degradation of PTFE even under the condition of low-dose irradiation [5].

Among the techniques available, treatment by low-temperature plasma under different conditions has been extensively employed to activate and improve the surface properties of PTFE without altering its bulk properties. However, the improved properties of plasma-treated PTFE, such as wettability, will gradually be lost with the elongation of time [6]. Aimed at overcoming the time-dependent effect of plasma treatment, graft polymerization of functional vinyl monomers onto a PTFE surface via a plasma pretreatment technique is a good choice, since it can introduce fresh and specific functional groups onto the PTFE surface [7, 8]. Many monomers, such as acrylic acid (AAc), 4-vinylpyridine, 1-vinylimidazole [9], glycidyl methacrylate [10], and acrylamide [11], have been graft-polymerized onto a PTFE surface in order to ameliorate its adhesion using a low-temperature plasma-induced grafting method.

In this work, the AAc monomer was selected and grafted onto the surface of a PTFE film via a low-temperature plasma technique. The influences of plasma power and treating time on the spin number of free radicals in PTFE film were investigated by analysis of the electron spin resonance (ESR) spectra; to the best of our current knowledge, this has never been referred to in the literature up to now. Attenuated total reflection Fourier transform infrared (ATR-FTIR) spectroscopy and X-ray photoelectron spectroscopy (XPS) were utilized to confirm the presence of grafted poly(acrylic acid) chains. Scanning electron microscopy (SEM) and atomic force microscopy (AFM) were employed to observe the surface morphology of PTFE films. The thermostability and hydrophilicity of PTFE films were evaluated by thermogravimetric analysis (TGA) and static water contact angle (WCA) measurements. Electrical properties were determined via measuring the dielectric constant ( $\epsilon_r$ ), dielectric loss ( $\tan\delta$ ), and surface electrical resistance ( $R_s$ ).

## 2 Materials and methods

### 2.1 Materials

PTFE film (thickness  $100 \pm 5 \mu\text{m}$ ) was provided by Guangdong Shengyi Technology Co., Ltd., China, and AAc was purchased from Sinopharm Chemical Reagent Co., Ltd., China. All of the chemicals in this work were of analytical grade and used without further purification.

### 2.2 Preparation of PTFE-g-PAAc film

The preparation process of PTFE-g-PAAc film is described in Fig. 1. PTFE film was pretreated with a low-temperature plasma (Changzhou Zhongkechangtai Plasma Science and Technology Co., Ltd., China) under an argon atmosphere and then put into a glass tube containing a deionized aqueous solution of AAc after placement in air for several minutes. AAc was graft-polymerized onto the PTFE film surface at  $70^\circ\text{C}$  under the protection of nitrogen to prepare PTFE-g-PAAc film. After that, the PTFE-g-PAAc film was fetched out and rinsed with deionized water to remove any homopolymers and remaining monomers. Eventually, the PTFE-g-PAAc film was dried in a vacuum drying oven at  $60^\circ\text{C}$  until the weight of the film became constant. The grafting density ( $GD$ ) was calculated by:

$$GD = (W_g - W_o)/A_o, \quad (1)$$

where  $W_o$  and  $W_g$  are the weights (in  $\mu\text{g}$ ) of the original PTFE and PTFE-g-PAAc films, respectively.  $A_o$  represents the area (in  $\text{cm}^2$ ) of the PTFE film.

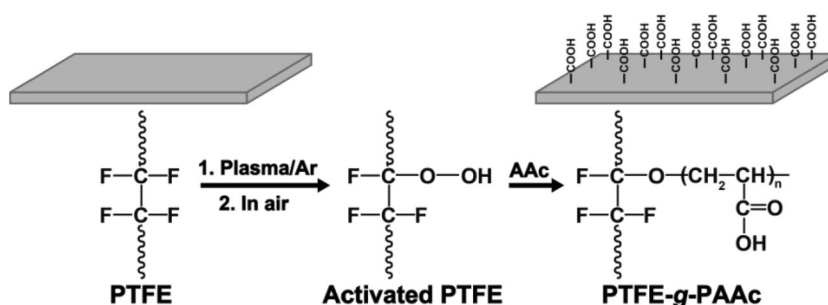
### 2.3 ESR measurements

The low-temperature plasma-treated PTFE films under argon atmosphere were put into quartz glass tubes ( $\Phi$ , 5 mm; length, 200 mm) for ESR measurements at room temperature with a Bruker EMX300 spectrometer (frequency, 9.65 GHz; power, 1 mW; field modulation frequency, 100 kHz). The direction of the PTFE films was maintained perpendicular to the ESR magnetic field. It should be noted that the PTFE films treated by the plasma were in contact with air for several minutes before ESR measurements. The spin number of free radicals was determined with the spectral double-integration method [12]. Five different points of the tested sample were determined to obtain a mean value of the spin number.

### 2.4 Characterization

The surface topography of the PTFE samples was investigated using SEM (FEI Quanta 250, USA). PTFE films were covered with a thin layer of gold before observation, and an acceleration voltage of 10 kV was used. An atomic force microscope (AFM) (Nanoscope V, Bruker Corp., USA) equipped with a J scanner was used to investigate the surface morphologies of the PTFE films. AFM images (scale  $20 \mu\text{m} \times 20 \mu\text{m}$ ) were obtained in the tapping mode. The nominal spring constant of the silicon nitride cantilevers (NSC-11, Bruker Corp., USA) used in this study was 0.24 N/m.

**Fig. 1** Schematic diagram of low-temperature plasma and Ar-pretreatment-induced AAc graft polymerization onto a PTFE film surface



The chemical structure of the PTFE films was analyzed according to Fourier transform infrared (FTIR) spectroscopy. FTIR spectra were acquired from 4000 to 650  $\text{cm}^{-1}$  on a Bruker Tensor 27 FTIR spectrometer in attenuated total reflectance mode by averaging eight scans at 4  $\text{cm}^{-1}$  resolution. The chemical composition of the PTFE specimens was investigated via XPS spectra. The investigations were carried out via a Kratos Axis Ultra instrument with monochromatic Al  $K\alpha$  radiation. XPS spectra were obtained through wide scans in the range of 1100–0 eV, and high-resolution spectra of the  $\text{C}_{1s}$  region were collected.

The thermal stability of the PTFE films was assessed by TGA on a TG 209 F3 Tarsus (NETZSCH, Germany) instrument. PTFE specimens were heated from 20 to 800  $^{\circ}\text{C}$  under nitrogen atmosphere with a heating rate of 10  $^{\circ}\text{C}/\text{min}$ .

The surface hydrophilicity of the PTFE films was evaluated by static WCA measurements using a KSV Theta Optical Tensiometer equipped with a digital camera (KSV Instruments Ltd., Finland). A drop of water (5  $\mu\text{L}$ ) was laid on the tested PTFE film surface. Five various points of each specimen were measured, and the WCA was the mean value of the acquired data.

## 2.5 Electrical properties

$E_r$  and  $\tan\delta$  of the PTFE films were determined at a frequency of 10 GHz by an Agilent N5230A vector network analyzer using a split post dielectric resonator (SPDR) method [13]. The relative humidity and temperature were controlled at 50 % and 23  $^{\circ}\text{C}$ , respectively.

$R_s$  ( $\Omega \text{ cm}^2$ ) of the PTFE films was determined using a sample cell made of Plexiglas<sup>®</sup> with two platinized platinum electrodes, two electrolyte chambers, and a GW INSTEK LCR-817 m with an accuracy of 0.05 %. The prepared square-shaped PTFE films (5 cm  $\times$  5 cm) were put into a KOH (30 wt%) deionized aqueous solution for more than 24 h and then immersed into the sample cell containing a KOH (30 wt%) deionized aqueous solution. The temperature of the sample cell, voltage, and frequency

were set at 25  $^{\circ}\text{C}$ , 1 V, and 1 kHz, respectively.  $R_s$  was calculated according to

$$R_s = (R_1 - R_0) \times A, \quad (2)$$

where  $R_1$  and  $R_0$  are obtained resistance ( $\Omega$ ) of the film immersed cell and the blank cell, respectively, and  $A$  is the sample surface area (in  $\text{cm}^2$ ).

## 3 Results and discussion

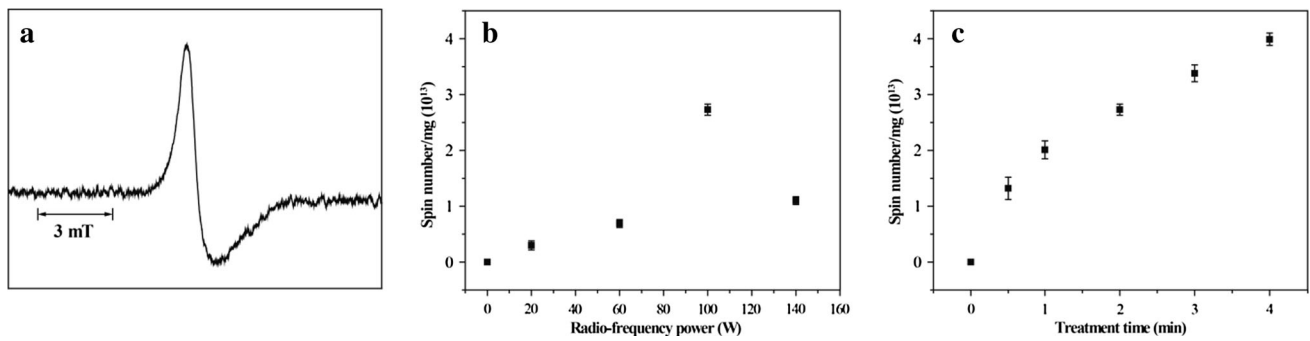
### 3.1 ESR measurements

Figure 2 shows the ESR spectrum and the spin number of free radicals in a PTFE film formed by plasma treatment under an argon atmosphere. The characteristic ESR spectrum shown in Fig. 2a belongs to the overlapping signals of peroxy mid-chain radicals and peroxy end-chain radicals, both of which are products of the reaction between free radicals and oxygen in air [14]. The emergence of the peak of the spin number depicted in Fig. 2b indicates that an appropriate radio-frequency power is more favorable to PTFE surface activation and the formation of peroxy radicals. Figure 2c indicates that the spin number logically increases with the extension of plasma treatment time.

### 3.2 Characterization of PTFE films

SEM pictures of the original PTFE and PTFE-g-PAAc ( $GD = 696 \mu\text{g}/\text{cm}^2$ ) films are illustrated in Fig. 3. As clearly illustrated in Fig. 3a, a', there are a number of nanopores distributed on the unmodified PTFE film surface. Compared with Fig. 3a, a', it can be obviously observed from Fig. 3b, b' that the surface nanopores have disappeared and the surface of the PTFE-g-PAAc film becomes rougher, indicating that PAAc chains are successfully immobilized on the PTFE film surface.

The surface topography of the pristine PTFE and PTFE-g-PAAc ( $GD = 696 \mu\text{g}/\text{cm}^2$ ) films is visualized by AFM. As is evident in Fig. 4, the PTFE-g-PAAc film surface is much rougher (Fig. 4b, b') than that of the neat PTFE film (Fig. 4a, a'). The surface roughness of the PTFE samples



**Fig. 2** **a** ESR spectrum of an argon-plasma-treated PTFE film. Effects of **b** radio-frequency power and **c** treatment time on the spin number of free radicals in PTFE film

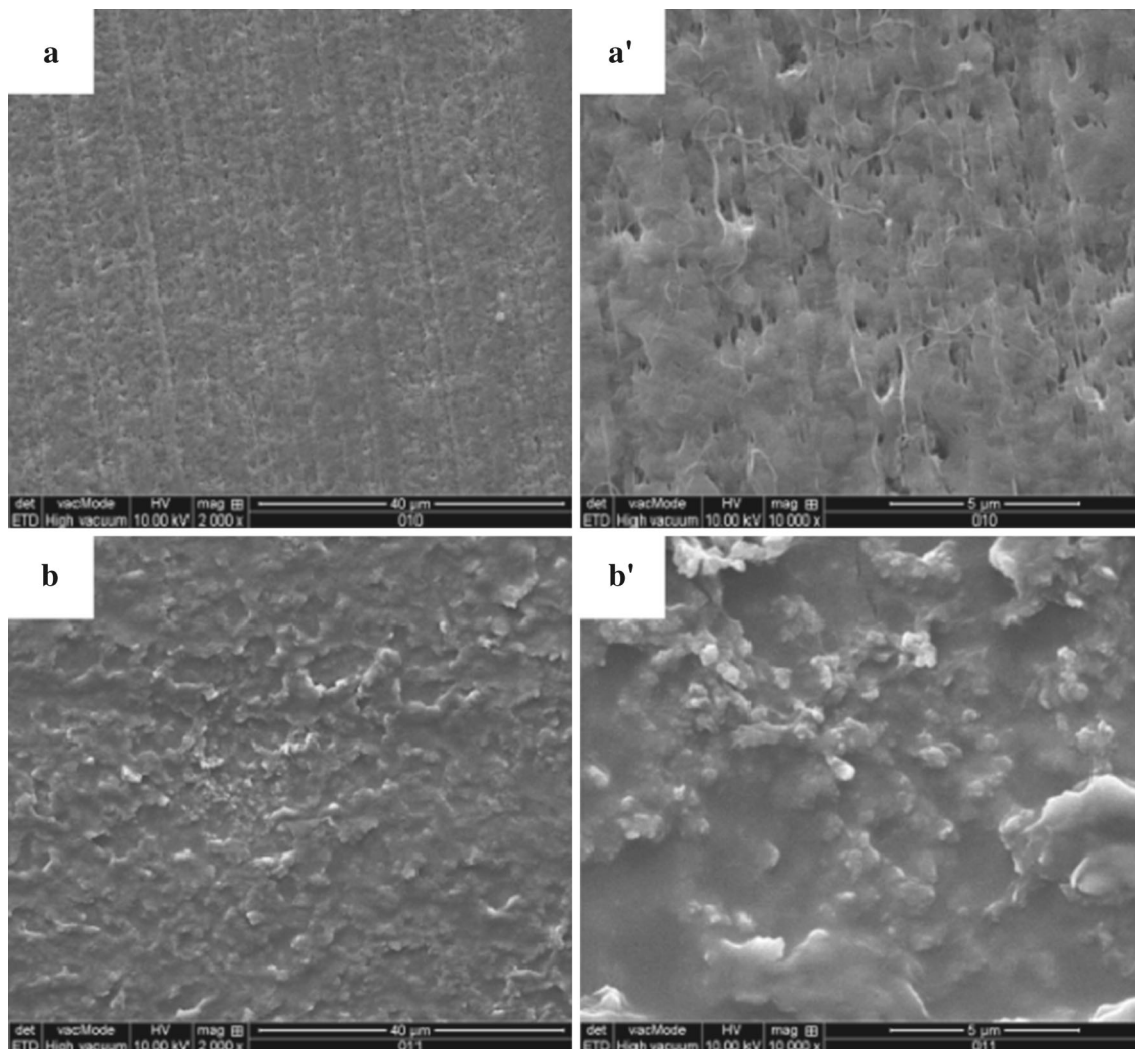


**Fig. 3** SEM images of the original PTFE (**a**  $\times 2000$ ; **a'**  $\times 10,000$ ) and PTFE-g-PAAc films (**b**  $\times 2000$ ; **b'**  $\times 10,000$ ) with  $GD = 696 \mu\text{g}/\text{cm}^2$

computed from AFM data is listed in Table 1 and estimated in terms of three parameters: the average surface roughness ( $R_a$ ), the root-mean-square roughness ( $R_q$ ), and the maximum distance between the peak and valley of the

roughness ( $R_{\text{max}}$ ) [15]. As seen in Table 1,  $R_a$ ,  $R_q$ , and  $R_{\text{max}}$  of the PTFE-g-PAAc film are correspondingly about 2.6, 2.7, and 2.4 times larger, respectively, than those of the unmodified PTFE film. Therefore, the surface roughness of



**Fig. 4** AFM images of the pristine PTFE (**a** 2D; **a'** 3D) and PTFE-*g*-PAAc films (**b** 2D; **b'** 3D) with  $GD = 696 \mu\text{g}/\text{cm}^2$

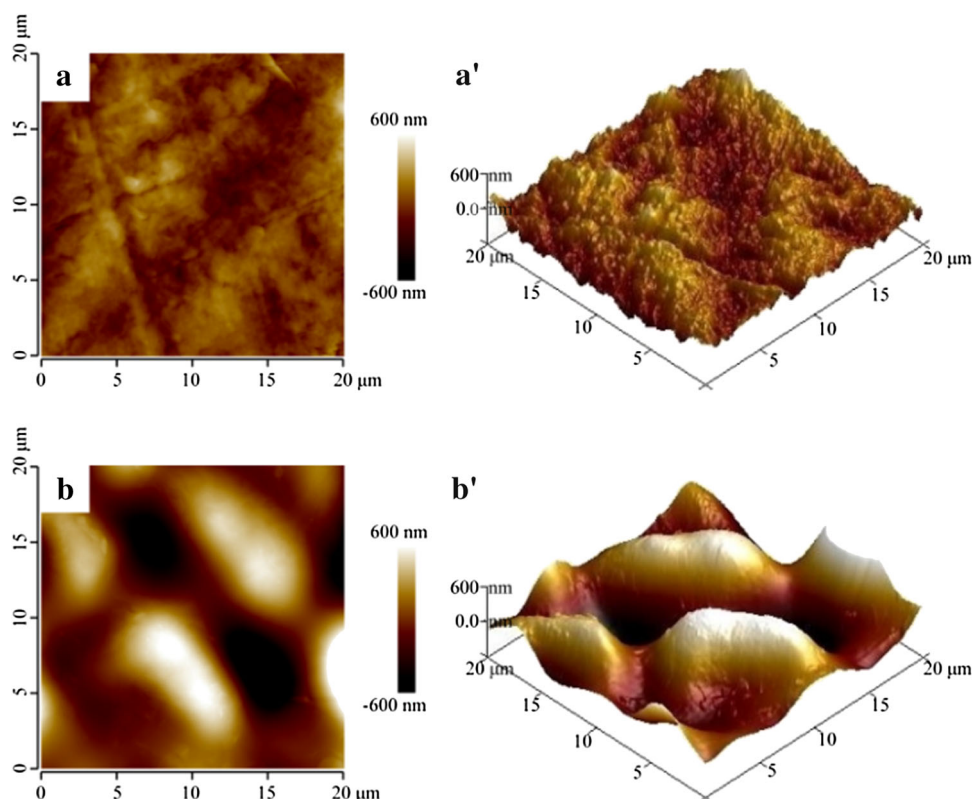


**Table 1** Surface roughness of the unmodified PTFE and PTFE-*g*-PAAc ( $GD = 696 \mu\text{g}/\text{cm}^2$ ) films

Sample	Surface roughness (nm)		
	$R_a$	$R_q$	$R_{\text{max}}$
Pristine PTFE	86.5	106	792
PTFE- <i>g</i> -PAAc ( $GD = 696 \mu\text{g}/\text{cm}^2$ )	221	283	1881

PTFE-*g*-PAAc film is effectively enhanced, which might be more convenient for adhesion to other materials.

ATR-FTIR spectra of the nascent PTFE and PTFE-*g*-PAAc films are shown in Fig. 5a. Compared with that of the original PTFE, a new peak at  $1697 \text{ cm}^{-1}$  can be seen from the spectrum of the PTFE-*g*-PAAc sample, which is attributed to the stretching vibrations of carboxyl group [16, 17]. XPS spectra of the virgin PTFE and PTFE-*g*-PAAc films are illustrated in Fig. 5b. The neat PTFE film exhibits two characteristic peaks, ascribed to  $\text{C}_{1s}$  (289.8 eV) and  $\text{F}_{1s}$  (687.0 eV), respectively. After graft modification, a fresh band at 532.1 eV ( $\text{O}_{1s}$ ) emerges on the curve of the PTFE-*g*-PAAc sample. In addition, the intensity of the  $\text{F}_{1s}$  peak is much weaker than that of the original PTFE specimen. As listed in Table 2, the F/C atomic ratio decreases from 2.71 (neat PTFE) to 0.34 (PTFE-*g*-PAAc), whereas the O/C atomic ratio increases from 0.01 (neat PTFE) to 0.59 (PTFE-*g*-PAAc). The high-

resolution  $\text{C}_{1s}$  spectra and  $\text{C}_{1s}$  components of the pristine PTFE and PTFE-*g*-PAAc films are illustrated in Fig. 5c, d, and Table 3, respectively. As we can see, Fig. 5c consists of a strong peak component at 292.3 eV, which represents  $\text{CF}_2$  (79.21 %) and a minor peak at 284.8 eV (20.79 %) ascribed to C–C. Compared to that of neat PTFE film (Fig. 5c), the  $\text{C}_{1s}$  peak of PTFE-*g*-PAAc film is fitted by four distinctive carbon moieties in Fig. 5d, which are C–C (284.8 eV, 41.92 %), C–O (286.1 eV, 13.89 %), O=C–O (288.8 eV, 26.07 %), and  $\text{CF}_2$  (291.8 eV, 18.12 %). The ATR-FTIR and XPS spectra further confirm that AAc is graft-polymerized onto the PTFE film surface.

The thermal stability of the pristine PTFE and PTFE-*g*-PAAc films is assessed via TGA. The TGA and DTG profiles are depicted in Fig. 6. TGA and DTG profiles of the pristine PTFE film show one decomposition step, and the initial decomposition temperature and the temperature of the maximum degradation rate are approximately 515 and 577 °C, respectively [18]. On the other hand, the thermodegradation of PTFE-*g*-PAAc film can be divided into two steps according to the TGA and DTG profiles. The temperatures of the maximum degradation rate are about 410 °C owing to the decomposition and carbonization of PAAc chains and 595 °C due to the degradation of the PTFE main chain. As compared with that of original PTFE film, the thermal stability of PTFE-*g*-PAAc film decreases very slightly, which can be ascribed to the comparatively

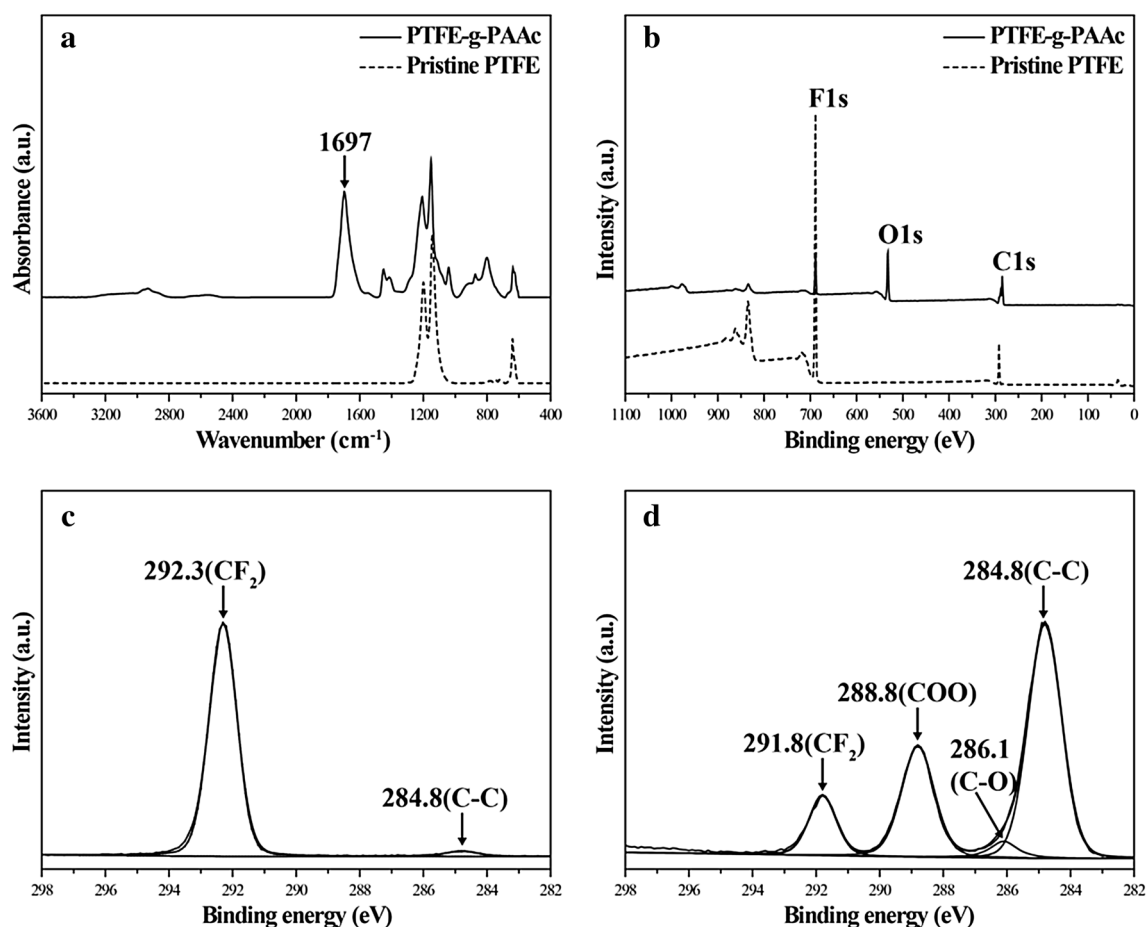


**Fig. 5** **a** ATR-FTIR and **b** XPS spectra of nascent PTFE and PTFE-g-PAAc ( $GD = 696 \mu\text{g}/\text{cm}^2$ ) samples.  $\text{C}_{1\text{s}}$  core-level spectra of **c** neat PTFE and **d** PTFE-g-PAAc samples [in **(d)**,  $GD = 696 \mu\text{g}/\text{cm}^2$ ]

**Table 2** Atomic contents of the pristine PTFE and PTFE-g-PAAc samples

Sample	Atomic percent (%)			Elemental ratios	
	C	F	O	F/C	O/C
Pristine PTFE	26.90	72.95	0.15	2.71	0.01
PTFE-g-PAAc ( $GD = 696 \mu\text{g}/\text{cm}^2$ )	51.31	18.28	30.41	0.34	0.59

**Table 3** Contribution of  $\text{C}_{1\text{s}}$  components (in %) to the neat PTFE and PTFE-g-PAAc samples

Sample	C-C	C-O	COO	$\text{CF}_2$
Pristine PTFE	20.79	—	—	79.21
PTFE-g-PAAc ( $GD = 696 \mu\text{g}/\text{cm}^2$ )	41.92	13.89	26.07	18.12

low thermal stability of the PAAc chain. Nevertheless, the thermal stability of bulk PTFE film remained nearly invariable after AAc graft modification.

WCA measurements have been extensively used to evaluate surface hydrophilicity of membranes [19].

Figure 7 depicts the static WCA of the neat PTFE and PTFE-g-PAAc ( $GD = 218 \mu\text{g}/\text{cm}^2$ ) films. Compared with the WCA ( $116^\circ$ ) of the original PTFE film, the WCA of the PTFE-g-PAAc sample decreases to  $78^\circ$ , indicating that the surface wettability of the PTFE-g-PAAc film is efficiently improved due to the introduction of carboxyl groups.

### 3.3 Electrical properties

Table 4 presents both dielectric properties ( $\epsilon_r$  and  $\tan\delta$ ) at 10 GHz and  $R_s$  of the virgin PTFE and PTFE-g-PAAc ( $GD = 218 \mu\text{g}/\text{cm}^2$ ) samples. Dielectric properties of polymeric materials are dependent on not only their intrinsic electrical properties, but also on their surface

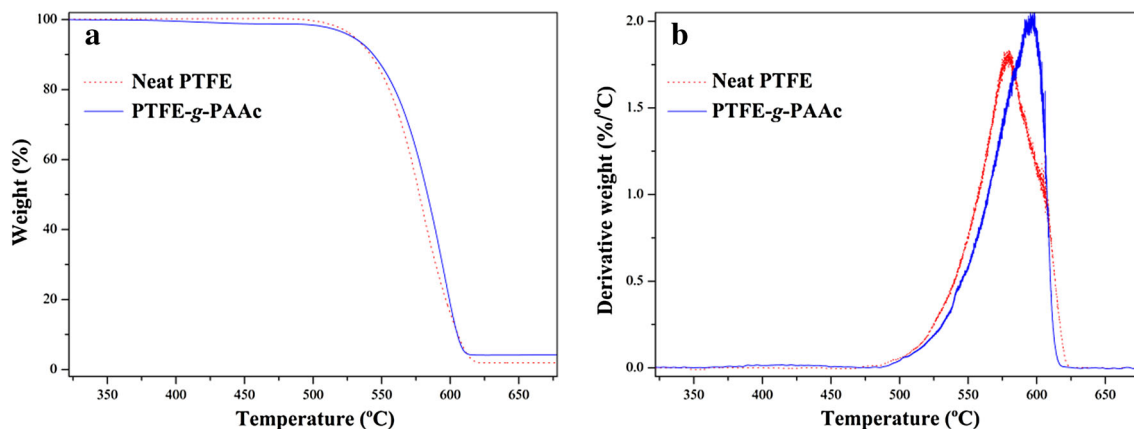


**Fig. 6** **a** TGA and **b** DTG profiles of the neat PTFE and PTFE-g-PAAc ( $GD = 696 \mu\text{g}/\text{cm}^2$ ) films in a  $\text{N}_2$  atmosphere

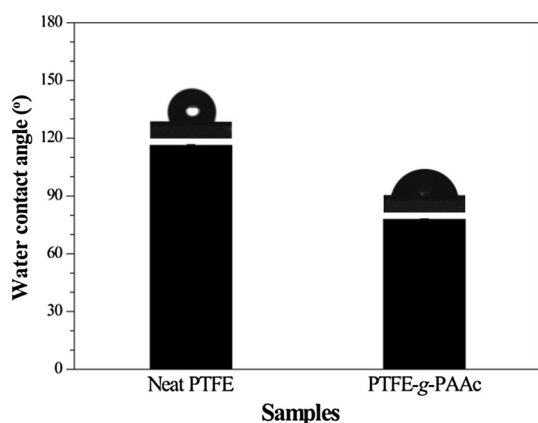


**Fig. 7** Water contact angle of the neat PTFE and PTFE-g-PAAc films ( $GD = 218 \mu\text{g}/\text{cm}^2$ )

composition and morphology [13]. Compared to that of the original PTFE film, the  $\epsilon_r$  of PTFE-g-PAAc film remains constant due to the fact that the performance of bulk PTFE film remains unchanged. On the contrary, the  $\tan\delta$  of the PTFE-g-PAAc film increases significantly from 0.0002 to 0.0073, since the introduction of carboxyl groups increases the polarity and moisture level of the PTFE film surface, both of which could result in energy loss. After AAc graft modification, the  $R_s$  of the PTFE-g-PAAc film is reduced slightly, from  $131.89$  to  $110.28 \Omega \text{ cm}^2$ , which is attributed to the fact that the grafted carboxyl groups, to some extent, improve the proton exchange capacity of PTFE film. However, PTFE-g-PAAc film maintains its inherent high-impedance performance because the AAc is only graft-

polymerized onto the PTFE film surface, not the interior of the PTFE film.

#### 4 Conclusion

Since the mechanical strength of expanded PTFE film is relatively poor, and UV irradiation combined with plasma pretreatment is somewhat complicated, in this study PTFE film was selected as the substrate and PTFE-g-PAAc film was successfully fabricated by a facile plasma-pretreatment-induced graft polymerization technique without the need of UV irradiation, which was proved by ATR-FTIR spectroscopy and XPS. The effects of radio-frequency power and treatment time of argon plasma on the spin number of free radicals in PTFE film were examined via ESR measurements in order to provide an appropriate plasma treatment process, which, to our knowledge, has not been previously reported in the published literature. Additionally, the peroxy radicals formed on the plasma-treated PTFE film were verified by examination of ESR spectra, which were used to initiate graft polymerization of AAc. Compared to that of the original PTFE film, the hydrophilicity of PTFE-g-PAAc film was effectively improved owing to the presence of PAAc grafting chains, which efficiently enhanced the compatibility between the PTFE film surface and other materials, such as epoxy resin, in the preparation of composite materials. The dielectric constant and surface electric resistance of PTFE-g-PAAc film were kept nearly constant after AAc graft modification, attributable to the fact that the PAAc chains were just

**Table 4** Electrical properties of the virgin PTFE and PTFE-g-PAAc films

Sample	$\epsilon_r/\tan\delta$	$R_s$ ( $\Omega \text{ cm}^2$ )
Virgin PTFE	$(2.03 \pm 0.03)/(0.0002 \pm 0.0000)$	$131.89 \pm 2.31$
PTFE-g-PAAc ( $GD = 218 \mu\text{g}/\text{cm}^2$ )	$(2.03 \pm 0.03)/(0.0073 \pm 0.0007)$	$110.28 \pm 1.88$

grafted onto the surface of the PTFE film. The synthesized PTFE-*g*-PAAc film could potentially be a promising material for the preparation of copper-clad laminates in the electronic industry, such as those used in printed circuit boards.

## References

1. C. Wang, J.R. Chen, Studies on surface graft polymerization of acrylic acid onto PTFE film by remote argon plasma initiation. *Appl. Surf. Sci.* **253**, 4599–4606 (2007). doi:[10.1016/j.apsusc.2006.10.014](https://doi.org/10.1016/j.apsusc.2006.10.014)
2. W.H. Yu, E.T. Kang, K.G. Neoh, Controlled grafting of comb copolymer brushes on poly(tetrafluoroethylene) films by surface-initiated living radical polymerizations. *Langmuir* **21**, 450–456 (2005). doi:[10.1021/la0485531](https://doi.org/10.1021/la0485531)
3. A. Venault, Y. Chang, H.H. Hsu et al., Biofouling-resistance control of expanded poly(tetrafluoroethylene) membrane via atmospheric plasma-induced surface PEGylation. *J. Membr. Sci.* **439**, 48–57 (2013). doi:[10.1016/j.memsci.2013.03.041](https://doi.org/10.1016/j.memsci.2013.03.041)
4. A. Zuzuarregui, B. Coto, J. Rodríguez et al., Highly reflective polymeric substrates functionalized utilizing atomic layer deposition. *Appl. Phys. Lett.* **107**, 061602 (2015). doi:[10.1063/1.4928375](https://doi.org/10.1063/1.4928375)
5. S.Y. Wu, E.T. Kang, K.G. Neoh et al., Surface modification of poly(tetrafluoroethylene) films by double graft copolymerization for adhesion improvement with evaporated copper. *Polymer* **40**, 6955–6964 (1999). doi:[10.1016/S0032-3861\(99\)00086-5](https://doi.org/10.1016/S0032-3861(99)00086-5)
6. S. Zanini, R. Barni, R. Della Pergola et al., Modification of the PTFE wettability by oxygen plasma treatments: influence of the operating parameters and investigation of the ageing behavior. *J. Phys. D Appl. Phys.* **47**, 325202 (2014). doi:[10.1088/0022-3727/47/32/325202](https://doi.org/10.1088/0022-3727/47/32/325202)
7. M.C. Zhang, E.T. Kang, K.G. Neoh et al., Consecutive graft copolymerization of glycidyl methacrylate and aniline on poly(Tetrafluoroethylene) films. *Langmuir* **16**, 9666–9672 (2000). doi:[10.1021/la000568l](https://doi.org/10.1021/la000568l)
8. Y.K. Cho, D. Park, H. Kim et al., Bioactive surface modifications on inner walls of poly-tetra-fluoro-ethylene tubes using dielectric barrier discharge. *Appl. Surf. Sci.* **296**, 79–85 (2014). doi:[10.1016/j.apsusc.2014.01.048](https://doi.org/10.1016/j.apsusc.2014.01.048)
9. S. Turmanova, M. Minchev, K. Vassilev et al., Surface grafting polymerization of vinyl monomers on poly(tetrafluoroethylene) films by plasma treatment. *J. Polym. Res.* **15**, 309–318 (2008). doi:[10.1007/s10965-007-9172-0](https://doi.org/10.1007/s10965-007-9172-0)
10. S.Y. Wu, E.T. Kang, K.G. Neoh et al., Surface modification of poly(tetrafluoroethylene) films by graft copolymerization for adhesion improvement with evaporated copper. *Macromolecules* **32**, 186–193 (1999). doi:[10.1021/ma9803133](https://doi.org/10.1021/ma9803133)
11. C.L. Li, C.Y. Tu, J.S. Huang et al., Surface modification and adhesion improvement of expanded poly(tetrafluoroethylene) films by plasma graft polymerization. *Surf. Coat Technol.* **201**, 63–72 (2006). doi:[10.1016/j.surfcoat.2005.10.041](https://doi.org/10.1016/j.surfcoat.2005.10.041)
12. Y.N. Zhao, M.H. Wang, Z.F. Tang et al., ESR study of free radicals in UHMW-PE fiber irradiated by gamma rays. *Radiat. Phys. Chem.* **79**, 429–433 (2010). doi:[10.1016/j.radphyschem.2009.11.007](https://doi.org/10.1016/j.radphyschem.2009.11.007)
13. Y. Yuan, Y.R. Cui, K.T. Wu et al., TiO<sub>2</sub> and SiO<sub>2</sub> filled PTFE composites for microwave substrate applications. *J. Polym. Res.* **21**, 366–371 (2014). doi:[10.1007/s10965-014-0366-y](https://doi.org/10.1007/s10965-014-0366-y)
14. K. Schierholz, U. Lappan, K. Lunkwitz, Electron beam irradiation of polytetrafluoroethylene in air: investigations on the thermal behavior. *Nucl. Instrum. Methods B* **151**, 232–237 (1999). doi:[10.1016/S0168-583X\(99\)00090-7](https://doi.org/10.1016/S0168-583X(99)00090-7)
15. N. Inagaki, K. Narushima, T. Amano, Introduction of carboxylic groups on ethylene-co-tetra fluoroethylene (ETFE) film surfaces by CO<sub>2</sub> plasma. *J. Adhes. Sci. Technol.* **20**, 1443–1462 (2006). doi:[10.1163/156856106778666417](https://doi.org/10.1163/156856106778666417)
16. Y. Yu, B.W. Zhang, X.X. Yang et al., Determining the degree of grafting for poly(vinylidene fluoride) graft-copolymers using fluorine elemental analysis. *Nucl. Sci. Technol.* **22**, 25–29 (2011). doi:[10.13538/j.1001-8042/nst.22.25-29](https://doi.org/10.13538/j.1001-8042/nst.22.25-29)
17. D.W. Jiang, C. Peng, Y.H. Sun et al., Study on technetium-99m labeling of graphene oxide nanosheets through click chemistry—<sup>99m</sup>Tc labeling of graphene oxide nanosheets. *Nucl. Sci. Technol.* **26**, 040301 (2015). doi:[10.13538/j.1001-8042/nst.26.040301](https://doi.org/10.13538/j.1001-8042/nst.26.040301)
18. J.F. Peng, J.Y. Qiu, J.F. Ni et al., Radiation synthesis and characteristics of PTFE-*g*-PSSA ion exchange membrane applied in vanadium redox battery. *Nucl. Sci. Technol.* **18**, 50–54 (2007). doi:[10.1016/s1001-8042\(07\)60018-9](https://doi.org/10.1016/s1001-8042(07)60018-9)
19. M.X. Hu, Q. Yang, Z.K. Xu, Enhancing the hydrophilicity of polypropylene microporous membranes by the grafting of 2-hydroxyethyl methacrylate via a synergistic effect of photoinitiators. *J. Membr. Sci.* **285**, 196–205 (2006). doi:[10.1016/j.memsci.2006.08.023](https://doi.org/10.1016/j.memsci.2006.08.023)